

10th ANKARA INTERNATIONAL AEROSPACE CONFERENCE
18-20 September 2019 - METU, Ankara TURKEY

AIAC-2019-176

COMPUTATIONAL FLUID DYNAMICS SIMULATIONS OF S76 ROTOR WIND TUNNEL TESTS

Osman Güngör¹
Turkish Aerospace
Ankara, Turkey

Murat Şenipek²
Turkish Aerospace
Ankara, Turkey

Alper Ezertaş³
Turkish Aerospace
Ankara, Turkey

ABSTRACT

The wind tunnel tests of S76 rotor were conducted by NASA. The test reports are open to public use hence results are valuable for validation studies of rotorcraft performance predictions using computational fluid dynamics. A rotor blade is subject to high speeds in the advancing side while retreating side suffers from reversed and strong separated flow. Moreover, overall rotor forces and moments must be trimmed to specified target while having flapping and lag freedom. Hence, CFD simulation of a rotor in forward flight is challenging problem at various aspects. The current study presents a solution methodology using commercial CFD software StarCCM+. The selected runs from test campaign are simulated in CFD environment. The S76 rotor performance predictions are compared with test results. The future studies are concluded to improve predictions.

INTRODUCTION

Forward flight simulation of rotorcrafts stands as a challenging problem for numerical aerodynamics however, numerical methods have evolved to state to analyze the designs and investigate the flow details. The accurate predictions of rotor performance assess the value of the methodologies. Hence, a validation study is carried out in the present work. S76 rotor system was tested by NASA and documentation is available for public use. The results of the test campaign are used in the comparative way.

Wind Tunnel Tests

Full scale wind tunnel tests of S76 rotor were conducted in NASA Ames 80x120 foot wind tunnel [Shinoda ve Johnson 1993] [Shinoda 1996]. Rotor performance and load data were provided for various rotor shaft angles, rotor loads and wind speeds from 0 to 100 knots. The 80x120 foot wind tunnel is open circuit tunnel and joint structure with 40x80 foot close circuit wind tunnel. The schematic of the both wind tunnels are provided in Figure 1. and 80x120 foot tunnel is highlighted in red. The test section is 80 feet in height, 120 feet in width and 493 feet in length.

¹ Design Engineer, Helicopter Group, Email: osman.gungor@tai.com.tr

² Design Specialist, Helicopter Group, Email: murat.senipek@tai.com.tr

³ Aerodynamic Chief Engineer, Helicopter Group, Email: aezertas@tai.com.tr

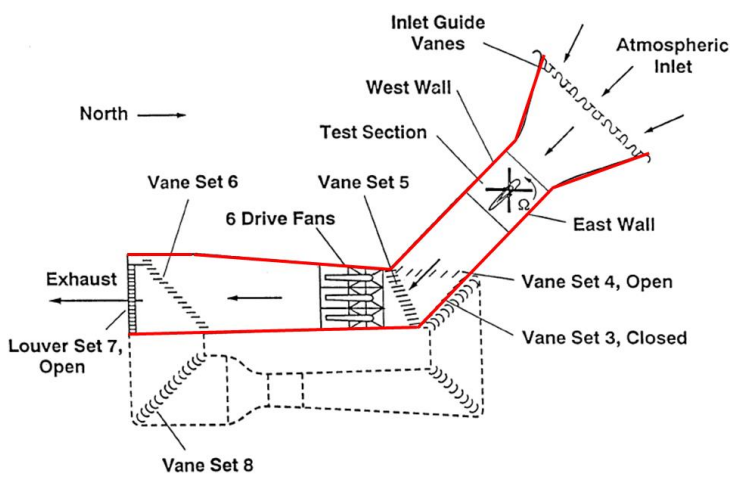


Figure 1 80x120 Foot Wind Tunnel Schematic and Wind Tunnel Model

The test rotor system is Sikorsky S-76 rotor system identical to production model and mounted on NASA modified Rotor Test Apparatus (RTA). The wind tunnel model is shown in Figure 1. The S-76 rotor system is articulated at the blade root by elastomeric bearings. Blade flap, lag and pitch are all achieved by same bearing. The main rotor parameters are listed in Table 1.

Table 1 S-76 Main Rotor Parameters [Shinoda 1996]

Parameter	Value	
Radius	6.70	m
Nominal Chord	0.3937	m
Nominal Twist	-10	deg
Blade Reference Area	10.56	m ²
Solidity Ratio	0.0748	
Number of Blades	4	
Airfoils	SC1095 from 84%	Radius
	SC1095R8 up to 80%	Radius
Flapping Hinge Offset	3.70%	Radius
Lock Number	11.6	
100% RPM	30.68	rad/s
100% Tip Speed	205.7	m/s

RTA is a test instrument specifically built for helicopter rotor test campaigns in the wind tunnels. RTA's testing limits are power of 3000 horsepower, thrust of 97800 N, and torque of 48800 Nm. The blade control system of RTA consists of three electro-hydraulic servo actuators connected to swashplate enabling collective and cyclic pitch controls. All tests in reported campaign are conducted with near zero trim of first harmonic of the rotor flapping.

METHOD

The test section and the rotor blades are included in the CFD model. As a part of wind tunnel, only test section is modelled with slip walls, inlet and outlet boundary conditions. Rotor test system is reflected through rotor blades and RTA having no slip boundary condition struts are excluded.

Commercial CFD package StarCCM+ is utilized in simulations. Coupled RANS solver with implicit unsteady time stepping is coupled with Spalart-Allmaras turbulence model. Curvature correction for turbulence model is also activated due to rotational characteristics of flow field. Second order discretization utilized in time and time step is selected such that rotor blades

advance 1 degree in azimuth-wise at each time step. In each time step, 10 inner iterations are performed. Second order upwind spatial discretization is employed for both flow and turbulence equations. For inviscid flux calculations, Roe's flux-difference splitting scheme is selected.

Overset meshing technique is utilized to ease the modelling of rotor blade motion. For each blade, a subdomain with polyhedral surface and volume elements is created. A back ground domain representing tunnel test section is discretized with Cartesian mesh. A refinement region encapsulating the blade subdomains is used in the background mesh. Element size of refinement region is selected such that wake of the rotor blades are sufficiently resolved. The coinciding elements of background mesh and boundary elements of subdomains should be in similar sizes in order to have minimum interpolation errors between overset and background regions. Hence, special attention is paid to element sizes of subdomain boundaries. A background mesh cutout, rotor blades, a subdomain and RTA geometry is presented in Figure 2. Since test section walls modelled as slip wall, prism layers are not generated however, for rotor blades and RTA geometry, 10 prism layers satisfying $y^+ > 30$ condition are employed.

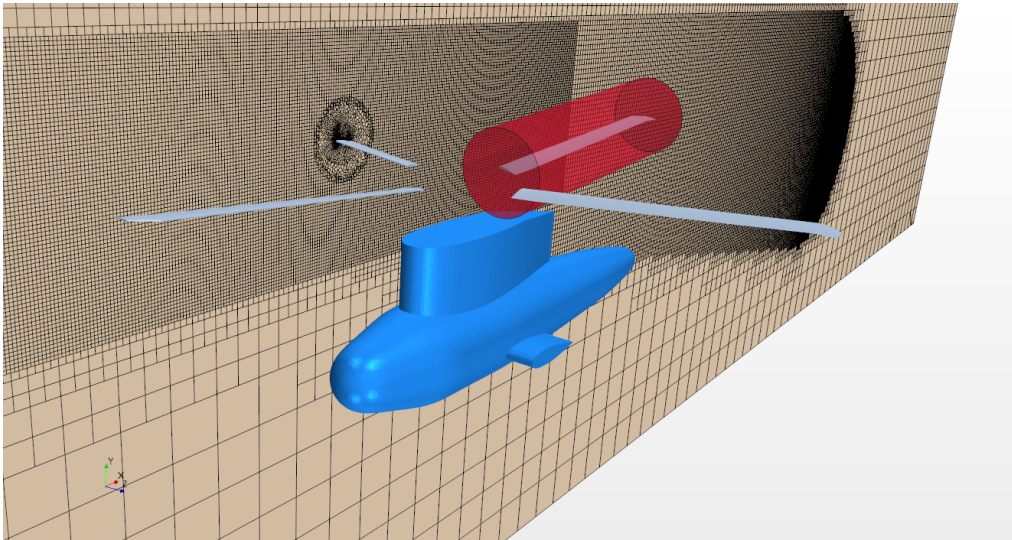


Figure 2 Background Mesh Cutout, Rotor Blades, Subdomain and RTA Geometry

Blade Motion

Rotation and harmonics of the rotor blade are introduced by following equations:

$$\psi^i = \omega t + \psi_0^i, \quad i = 1, 2, \dots, N_B \quad (I)$$

where ψ is instantaneous azimuth angle, ψ_0 is initial blade position, ω is rotational speed, t is time and N_B is the number of blades.

$$\theta^i(\psi) = \theta_0 - \sum_{n=1}^N (\theta_{nc} \cos n\psi^i + \theta_{ns} \sin n\psi^i), \quad i = 1, 2, \dots, N_B \quad (II)$$

where θ is instantaneous pitching angle, θ_0 is collective angle, and θ_{nc} and θ_{ns} are pitching harmonics.

The simplified flapping dynamics equation given below is solved for each blade. The angular acceleration around the flapping hinge is obtained. Time integration of flapping acceleration is performed to obtain flapping rate which is introduced into StarCCM+.

$$\ddot{\beta} + \left(1 + \frac{eM_b}{I_b} + \frac{\kappa_\beta}{I_\beta \omega^2} \right) \omega^2 \beta = \frac{M_{Aero}}{I_\beta} + \kappa_\beta \dot{\beta}$$

Rotor Trim

The rotor trim algorithm is developed in Java environment such that rates of collective and cyclic control angles are used as inputs to reach desired trim targets. A multidimensional Newton-Raphson iterator is integrated to solve target inputs. The trim targets are computed using 4 per revolution averages.

RESULTS

Predefined Motion Analyses

Performance data for forward flight thrust and speed sweep conditions with minimized flapping trim are presented at different shaft angles without any wall correction [Shinoda 1996]. The validation case is selected as run 48 of the tests. The run 48 is performed with 0 degree shaft angle starting from 5.2 knots to 100 knots then back to 4.8 knots. The integrated forces and moments of rotor are available for validation purposes. Moreover, dynamic loads presented as mean and peak-to-peak values are also documented. The blade control angles, collective and cyclic pitch, are also tabulated hence directly integrated into CFD simulations.

The CFD simulations are run for 5 full rotor revolutions. Integrated forces and moments are calculated for all blades. Key performance parameters, thrust and torque are tracked through the simulation. The thrust and torque coefficient history for a sample case is provided in Figure 3. The 4 per revolution fluctuations are observed after one revolution of the blade. Overall thrust and torque values are computed using one per revolution averaging over real time results.

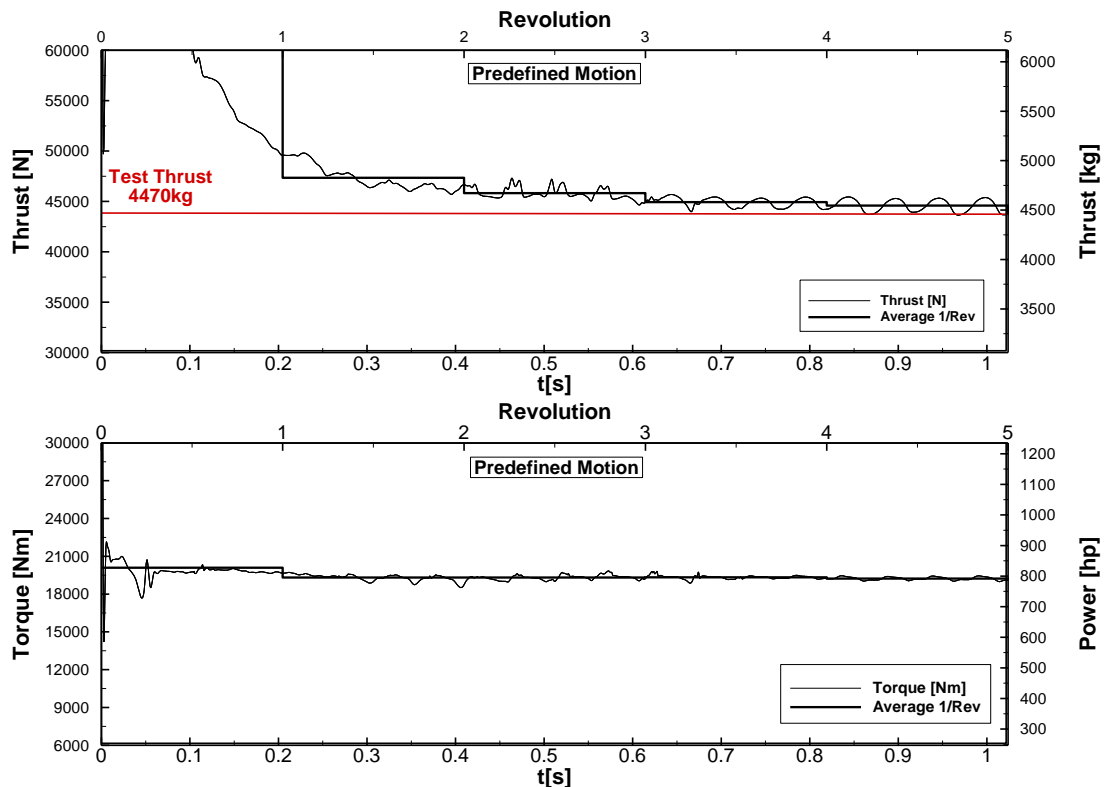


Figure 3 Sample Thrust and Torque History

Series of CFD simulations tabulated in Table 2 are conducted using the blade control angles provided in test report. Thrust and power coefficients are calculated and compared with test in Figure 4. During the tests, rotor system was trimmed to a constant thrust coefficient while minimizing 1st harmonics of flapping motion. In CFD simulations, blade angles are directly introduced according to wind tunnel test results. At low speeds with predefined motion, thrust

is excessive of target thrust however, it has a declining trend with increasing forward speed. Hence, results are not just incompatible but also have different trends which does not allow to make any conclusion. Similar trend is observed in power comparison.

Table 2 Analyses Conditions

Target Thrust		Airspeed	
Thrust [kg]	Thrust Coef. $\frac{C_T}{\sigma}$	Airspeed [Knots]	Advance Ratio, μ
4470	0.08	5	0.013
4470	0.08	20	0.050
4470	0.08	60	0.124
4470	0.08	80	0.200
4470	0.08	100	0.250

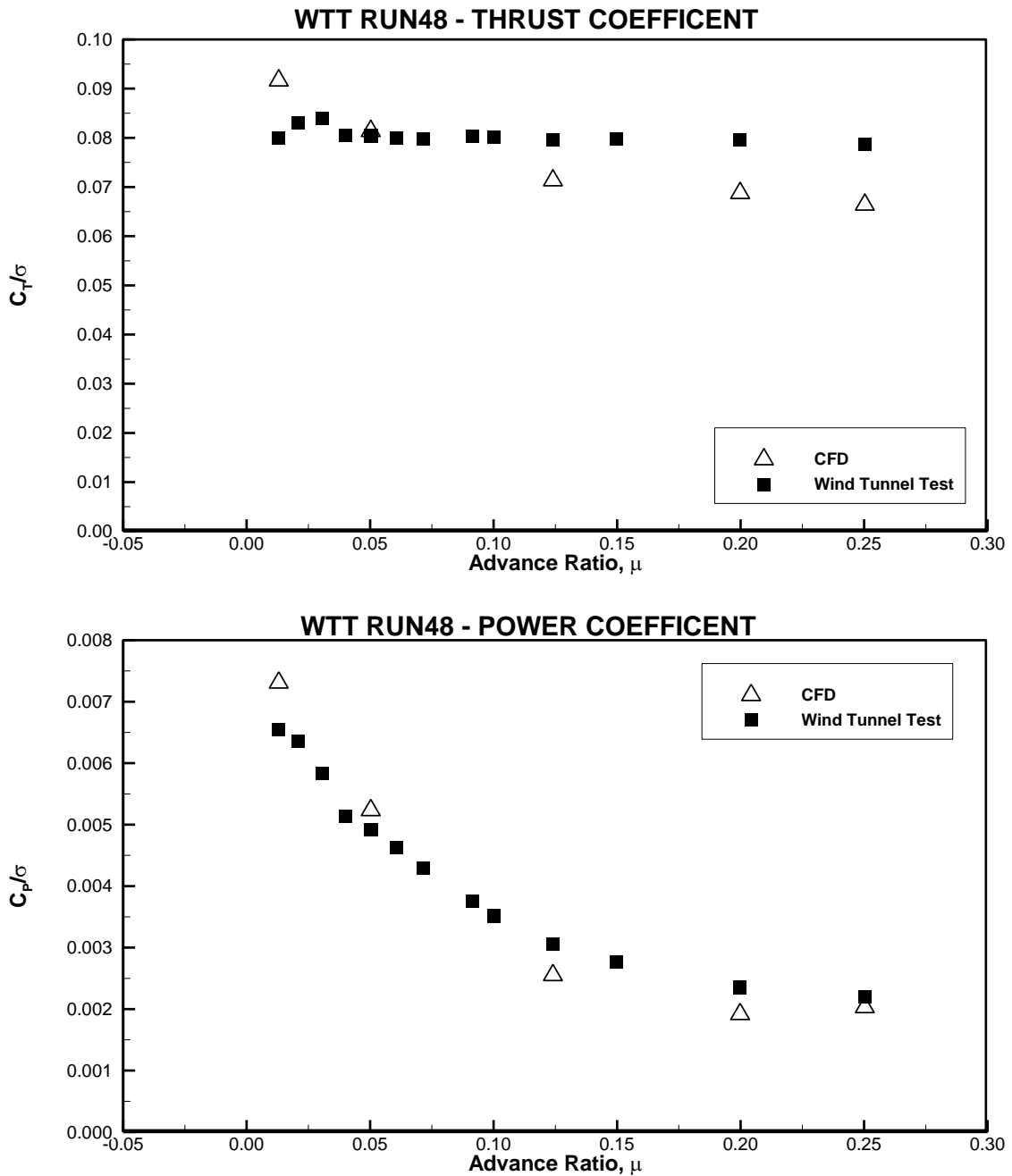


Figure 4 Thrust and Power Coefficient Comparison [Shinoda 1996]

Trim Analyses

The run 48 analyses are repeated in CFD environment with trimming approach presented in method section. Beside the key rotor performance parameters thrust and power, hub roll and pitch moment and blade flapping and control angles are also monitored to track solution convergence. The analyses are started with predefined control and flapping angles and run for 1 revolution. The trim algorithm is initiated after 1 revolution. Convergence is achieved within 10 full rotor revolutions. A sample analyses history is presented in Figure 5. Figure 7 shows a snapshot of flow field for a converged solution. The wake structure becomes fully developed and well resolved.

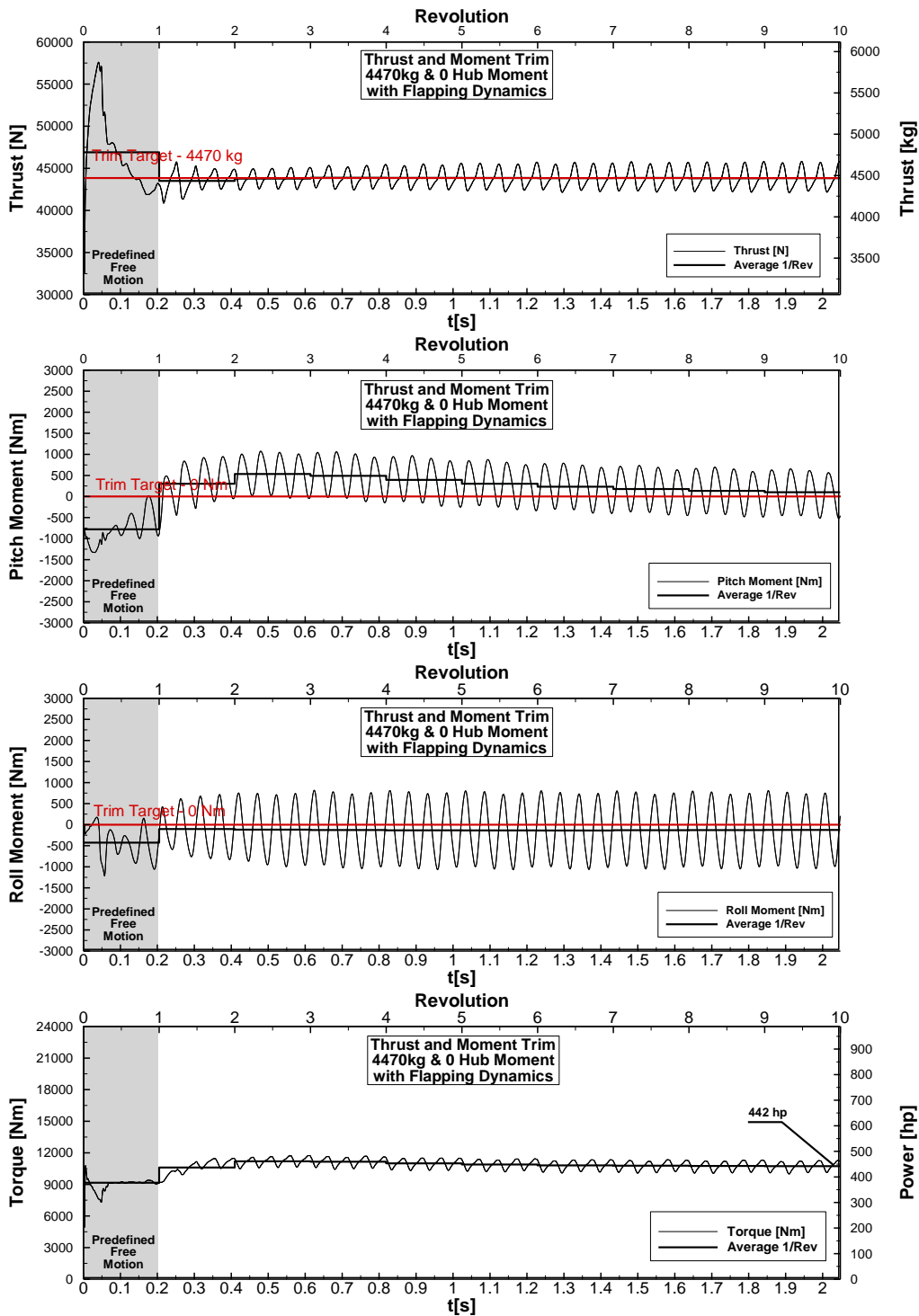


Figure 5 Sample Trim History - Moment and Forces

Trim algorithm reaches thrust target within 2-3 revolutions however, moment convergence trend is gradual. The rotor torque is highly responsive to thrust changes while effect of moment is weaker. However, progressive relation is observed between torque and moment variations hence convergence is needed to be observed at all targets to read required torque. The blade angles and first harmonics are presented in Figure 6. The first harmonics of the blade angles are extracted from individual blade angle histories using harmonic decomposition. The flapping dynamics synchronize to periodic environment of the forward flight within 1 revolution and changes in harmonics are minimal through analysis. The collective control angle shows similar trend to thrust history, similarly, cyclic control angles are consistent with hub moment histories.

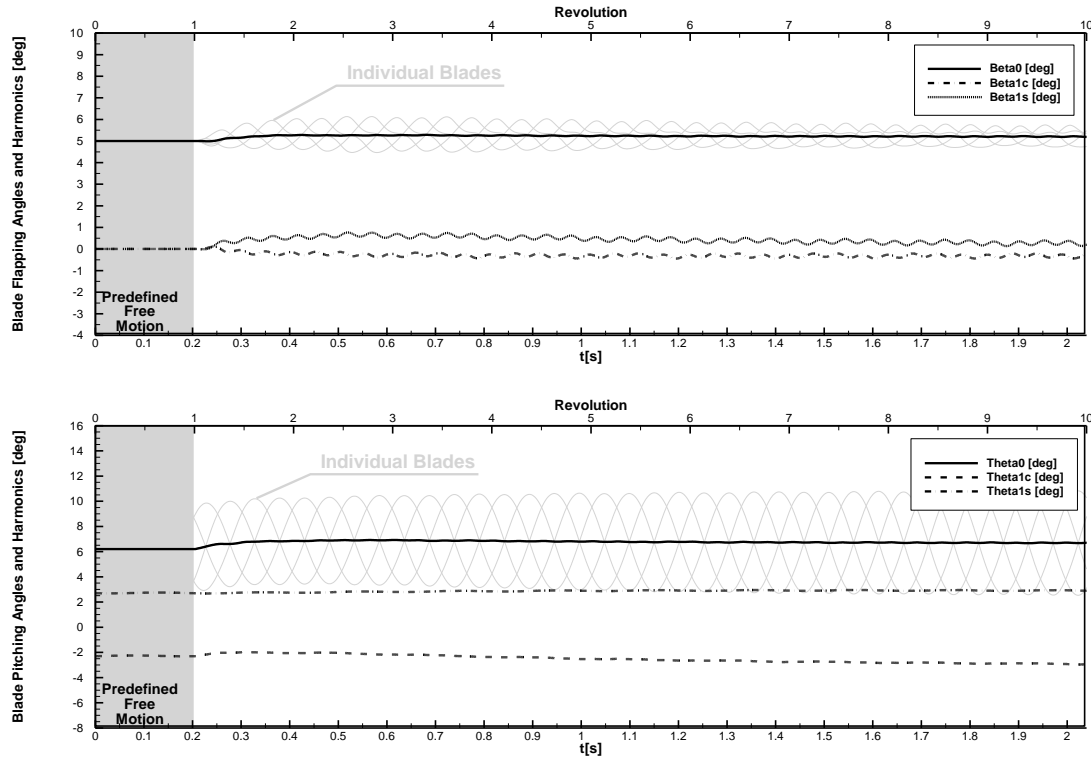


Figure 6 Sample Blade Control and Flapping Angles History

The key performance parameters, thrust and torque, are compared with test data in Figure 8 and Figure 9. The comparison data includes solutions with predefined blade angles, trim analyses only with rotor geometry and trim analyses with rotor and RTA geometry. Thrust comparison with predefined blade angles is provided to show how solution are deviated from target thrust and why trim algorithm is needed. Target thrust is successfully achieved at all trim analyses. The power predictions of the trim analyses are found to be satisfactory for engineering purposes. The near hover and highest air speed run results show slight deviations from test results. The solution grid provided in Figure 2 is prepared to resolve wake of the rotor in forward flight cases, hence it may be lacking grid refinement to accurately predict hovering performance where rotor wake directly convects downward.

The effect of RTA on rotor performance is also investigated. At low airspeeds, presence of RTA distorts the rotor wake and alters the pressure field, however interaction with RTA dies out with increasing airspeed. Additional important point is that blockage ratio of the wind tunnel section also differs with the presence of RTA. Slight required power difference is observed at the low speed analyses. Other than 5 knots, interaction with RTA is not present hence required power readings are almost identical.

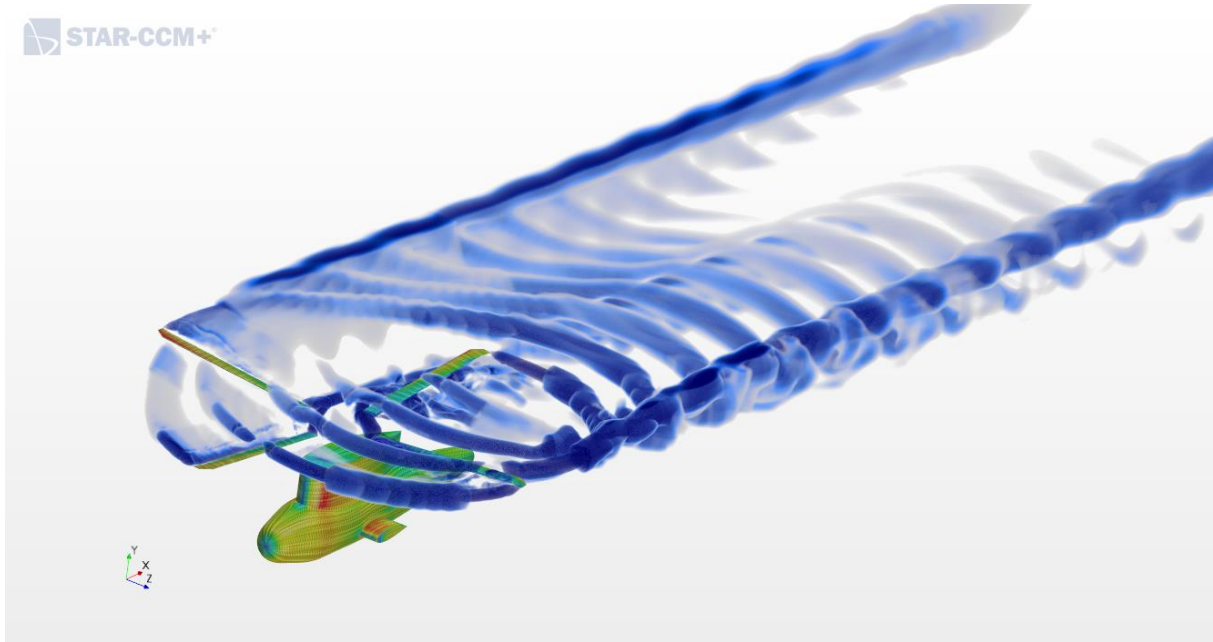


Figure 7 Wake Geometry in Advance Ratio of 0.25, Rotor Blades and Fuselage Colored with Velocity Magnitude

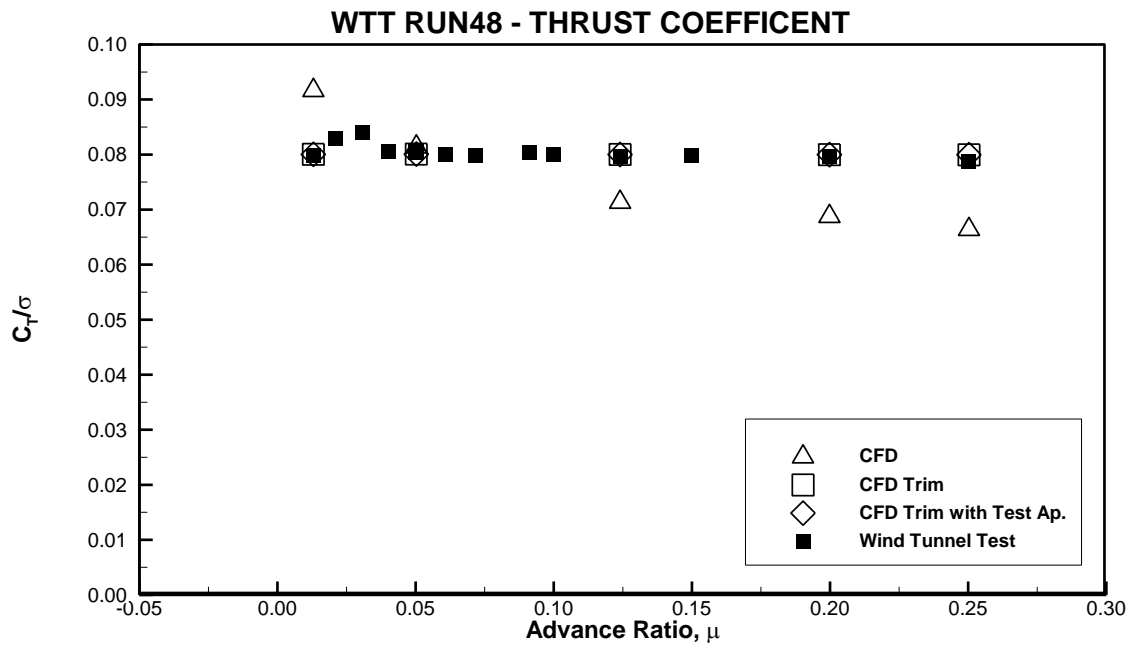


Figure 8 Advance Ratio vs Thrust Coefficient [Shinoda 1996]

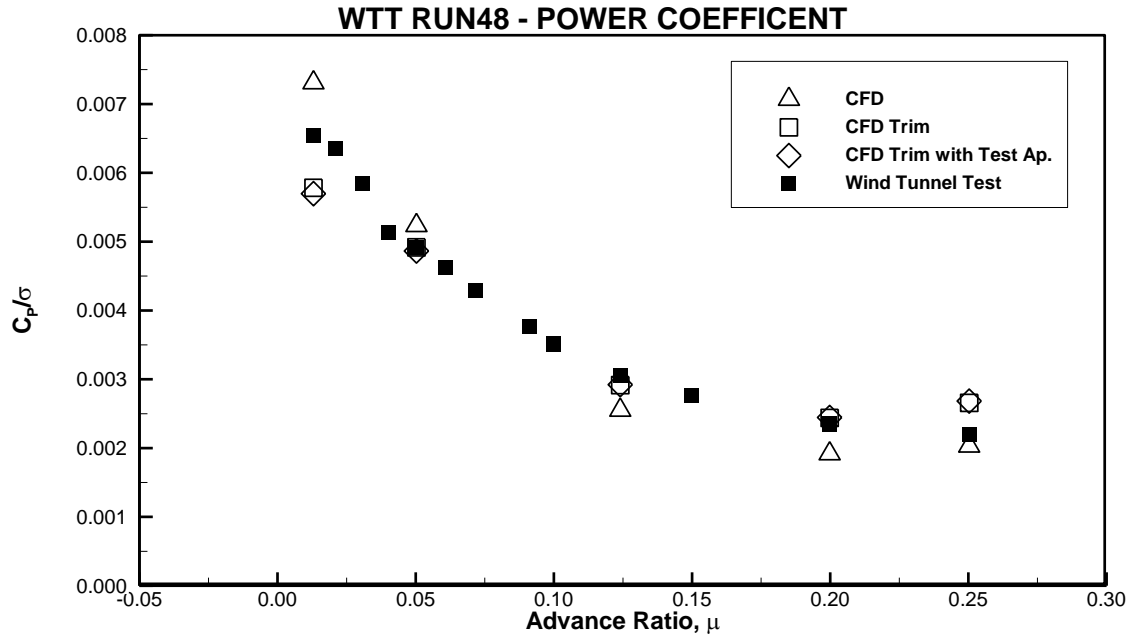


Figure 9 Advance Ratio vs Power Coefficient [Shinoda 1996]

The blade control and cone angle are presented from Figure 10 to Figure 13. The variation between collective control angle from analysis and test values are nearly in the range of 1 degree however, trends are observed to be similar. The cone angle results are also observed to be deviated around 1 degree at low speed, however deviation dies out with increasing air speed. In reality, rotor blades are elastic and there is a known elastic phenomenon of bending-torsion coupling. Hence, it would be meaningful to examine collective control angle and cone angle together. The airloads are clustered toward to tip of the blade at hovering and low speed flights, therefore blades are subject to higher bending moments. For a conventional rotor blade structure, increased bending deflection results in torsion in pitch down direction. Hence, sectional angle of attack distribution is reduced. In order to reach target thrust, higher collective control angle is required compared to rigid blade. In the same manner, due to bending deflections, smaller flapping angles are expected from elastic blades.

Other than lateral control angle, test and analysis results are consistent. Test trend is observed such that lateral control angle increases up to a certain speed then decreases at high speeds. However, analyses keep increasing trend from lowest to highest speed. Moreover, blade pitch angle histories for one revolution of blade is plotted in Figure 14. The pitch angle history shows that numerical model requires higher blade angles near 0 azimuth. In other words, blades have poor performance compared to real blades. The contradiction is suspected from the absence of the rotor hub in the analyses model. The rotor hub reduces the air speed and interacts with vortex trailing behind. Hence, numerical blade model might suffer from amplified yawed flow and vortex interactions.

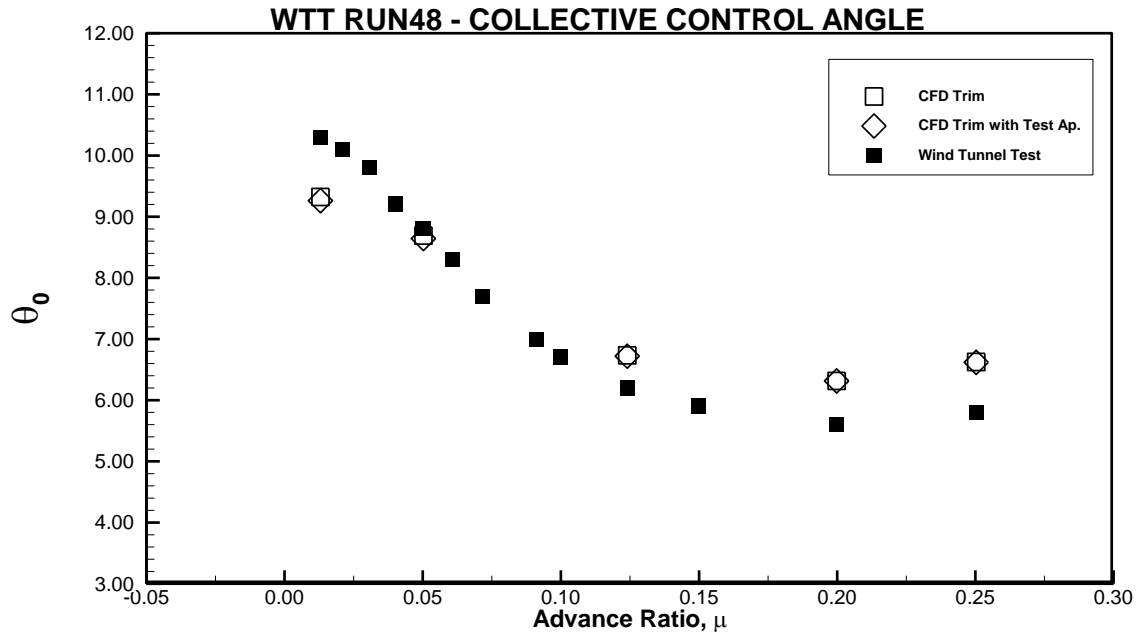


Figure 10 Advance Ratio vs Collective Control Angle [Shinoda 1996]

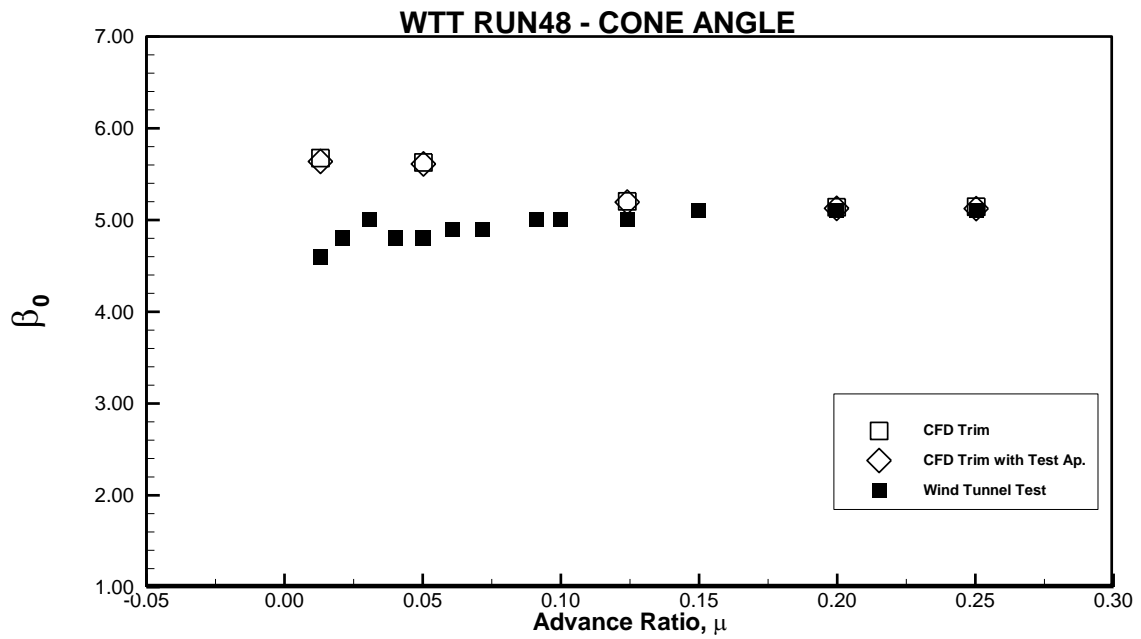


Figure 11 Advance Ratio vs Coning Angle [Shinoda 1996]

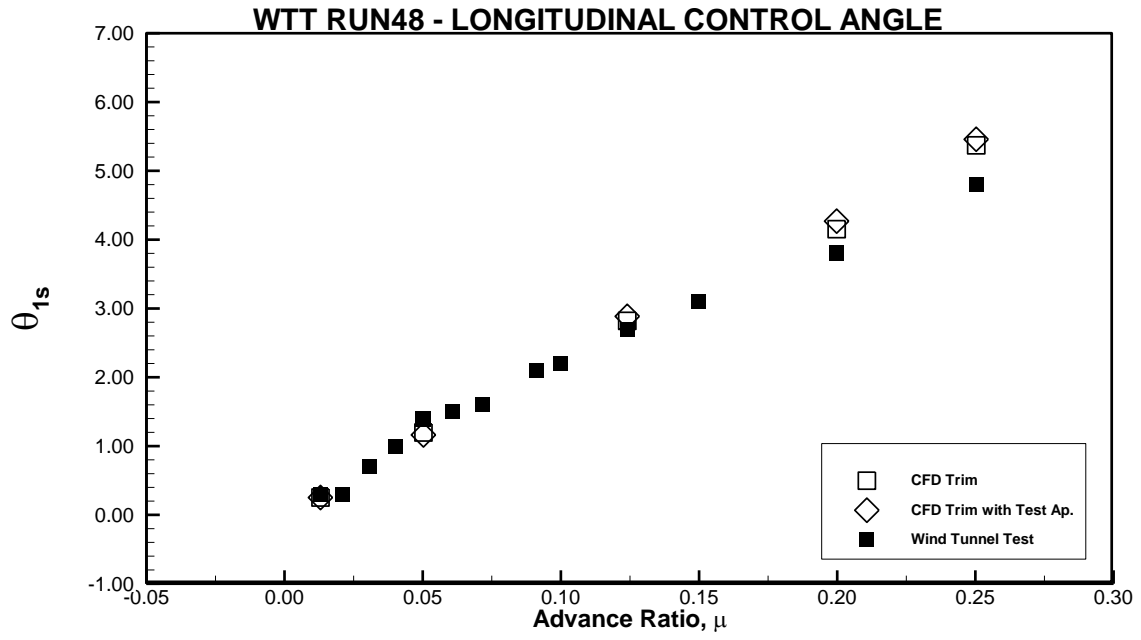


Figure 12 Advance Ratio vs Longitudinal Control Angle [Shinoda 1996]

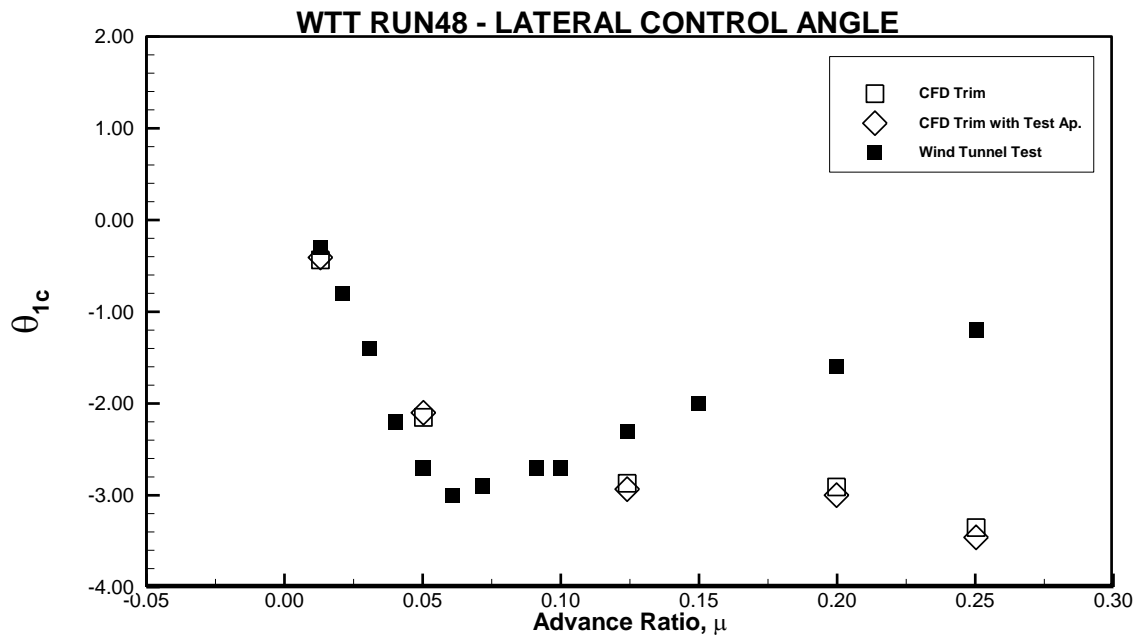


Figure 13 Advance Ratio vs Lateral Control Angle [Shinoda 1996]

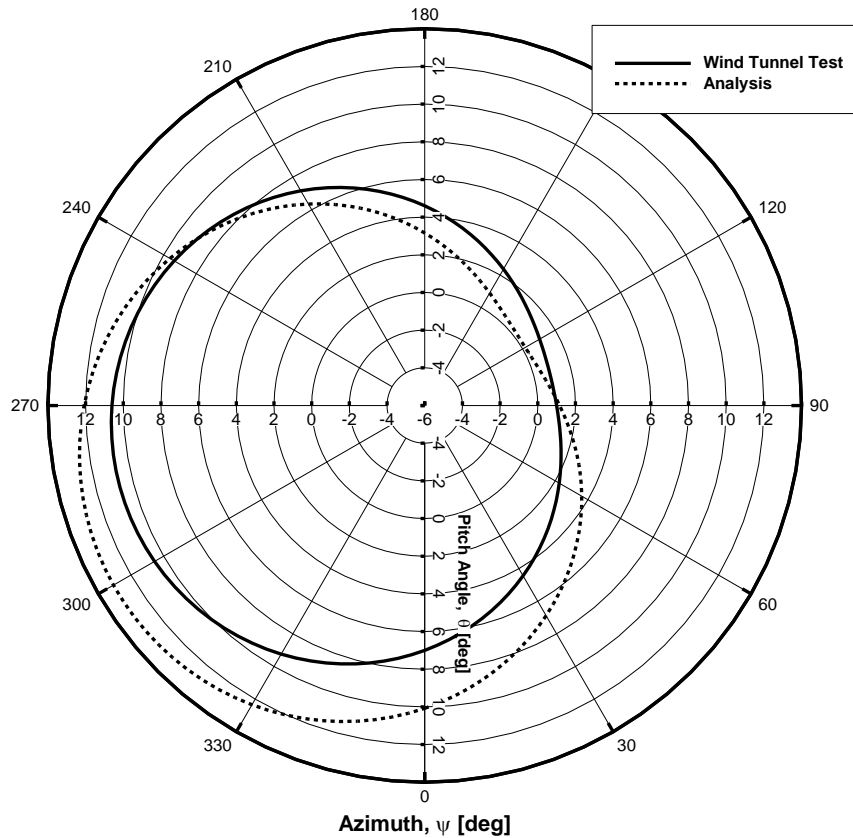


Figure 14 Blade Pitch Angle Variation at Advance Ratio of 0.25 [Shinoda 1996]

REMARKS

Forward flight simulation methodology presented through the document is validated against well-documented full scale rotor test results. Modelling approach is briefly explained. Initially, test and numerical model with predefined motion is compared. The deviation of results addresses the need for trimming of rotor in CFD environment. The analyses are repeated with trimming algorithm. Overall, satisfactory results are attained for prediction of rotor forward flight performance. However, undesired deviations are observed at some test points. To solve issues with inconsistent results, future studies planned are listed below as follows:

- Adaptive meshing strategy to be employed in order to capture flow field in high resolution from hover to high speed cases
- Effect of the hub geometry evaluation on the performance of rotor in high speed cases
- The elastic blade model to include elastic effects in the analyses to increase the fidelity of the presented approach.

The test document do not present any validation data related with flow field. Hence validation of predicted flow parameters could not be carried on.

References

- Shinoda, Patrick M. 1996. *Full-Scale S-76 Rotor Performance and Loads at Low Speeds in the NASA Ames 80-by 120-Foot Wind Tunnel*. NASA.
- Shinoda, Patrick M., and Wayne Johnson. 1993. "Performance Results from a Test of an S76 Rotor in the NASA Ames 80- by 120- Foot Wind Tunnel." *American Institute of Aeronautics and Astronautics*.